

Exploiting Hidden Block Sparsity: Interdependent Matching Pursuit for Cyclic Feature Detection

Yu Wang*, Wei Chen^{†*} and Ian J. Wassell*

* Computer Laboratory, University of Cambridge, UK

[†] State Key Laboratory of Rail Traffic Control and Safety, Beijing Jiaotong University, 100044, China
yw323@cam.ac.uk, weich@bjtu.edu.cn, ijw24@cam.ac.uk

Abstract—In this paper, we propose a novel Compressive Sensing (CS)-enhanced spectrum sensing approach for Cognitive Radio (CR) systems. The new framework enables cyclic feature detection with a significantly reduced sampling rate. We associate the new framework with a novel model-based greedy reconstruction algorithm: interdependent matching pursuit (IMP). For IMP, the hidden block sparsity owing to the symmetry present in the cyclic spectrum is exploited which effectively reduces the degree of freedom of problem. Compared with conventional CS with independent support selection, a remarkable spectrum reconstruction improvement is achieved by IMP.

I. INTRODUCTION

IN the cognitive radio (CR) regime, cognitive users (CUs) intelligently monitor and scavenge the holes in spectrum to improve the spectrum utilization. To reduce the interference to the primary users (PUs), CUs must be sensitive enough to detect weak primary signals drowned in noise. Feature detection is superior compared with its energy detection counterpart, regarding its ability to differentiate the PUs from white noise. For example, a cyclostationarity detector identifies the primary signal by exploiting its periodic characteristics [1], hence exhibiting robustness against the severe stationary white noise.

To enhance the spectrum sensing capability of a cyclostationary CR detector, compressive sensing (CS) has recently been employed that goes beyond the Shannon-Nyquist sampling paradigm [2]. Tian et al. contribute in the pioneering work [3] to linearly connect the sub-Nyquist measurements with the desired cyclic statistics in a CS framework. Sequentially, with the aim to reduce computational complexity, Rebeiz et al. propose to merely reconstruct the peak values of the spectral correlation density (SCD) matrix [4] by using the SCD estimator in [3]. In [5], Khalaf et al. consider the case that the cyclic frequencies of two consecutive time slots share the same nonzero supports and implement parallel CS reconstruction based on a joint detection among slots.

However, most of those existing CS-CR cyclic detectors resort to a recast optimization problem without considering remedies for the nontrivial computational difficulties. In [4], although only a part of the SCD is reconstructed to reduce the problem size, the recast l_2 norm problem is not guaranteed to yield the unique sparsest solution.

The work of Wei Chen is supported by the State Key Laboratory of Rail Traffic Control and Safety (No. RCS2012ZT014), Beijing Jiaotong University, and the Key grant Project of Chinese Ministry of Education (No.313006).

Taking into account these challenges, we propose a novel spectrum sensing framework to recover cyclostationary spectrum from CS measurements. The new framework bypasses the use of the auxiliary autocorrelation matrix or any mapping matrices which are critical for the framework in [3]. Particularly, since in [3] the symmetric components in the auxiliary autocorrelation matrix are discarded to reduce the problem dimension, severe spectral tails are incurred. We instead apply an average periodogram approach and benefit from interdependency among the symmetric supports, to reach the same goal of reducing the degree of freedom. We show that spectral tails in the SCD matrix are effectively suppressed by the proposed approach, which leads to higher accuracy and reliability for the sparsity-enforcing reconstruction. Furthermore, inspired by the model-based CS [6], we incorporate the characteristics of the proposed SCD estimator to facilitate the spectrum reconstruction and propose a novel model-based CS algorithm: Interdependent Matching Pursuit (IMP). In contrast to the existing algorithms that follow the conventional CS approach, IMP exploits hidden block sparsity among the symmetric spectral supports and effectively reduces the risk of reconstruction artifacts and false detection. Simulations show that the proposed framework with IMP has substantially lower mean square error (MSE) concerning the spectrum reconstruction and also higher probability of spectrum detection than the state-of-art. We further show that the model-based IMP is more robust against noise than the OMP, especially in the case where highly compressed measurements are provided.

The notation used is as follows. The superscripts $(\cdot)^H$, $(\cdot)^*$, $(\cdot)^T$, $(\cdot)^{-1}$ and $(\cdot)^\dagger$ denote complex conjugate-transpose, complex conjugate, transpose, inverse and Pseudo-inverse of a matrix respectively ($\mathbf{X}^\dagger = (\mathbf{X}^H \mathbf{X})^{-1} \mathbf{X}^H$). Bold $\{\mathbf{X}_k\}$ ($k = 1, 2, \dots, K$) denote a group of matrices. \otimes and $*$ correspond to Kronecker product and convolution respectively. $\|\cdot\|_p$ denotes the l_p norm for a vector and $\text{vec}(\mathbf{X})$ vectorizes matrix \mathbf{X} by sequentially concatenating columns into a vector. $\mathbf{X}[i]$ is the i th column of \mathbf{X} and $\mathbf{X}[J]$ the J th block of \mathbf{X} . $\bar{\mathcal{J}}$ denotes the complement of set \mathcal{J} . $\text{mod}(x, y)$ computes the modulus of x/y and $\lfloor x \rfloor$ floors x as an integer towards negative infinity.

II. SYSTEM MODEL AND PROBLEM FORMULATION

A. Compressive Sensing (CS)

We consider a discrete-time signal $\mathbf{y} \in \mathbb{C}^N$ which is sparse in some sparsifying basis $\Psi \in \mathbb{C}^{N \times N}$. The signal \mathbf{y} can be

linearly expressed as:

$$\mathbf{y} = \Psi \mathbf{s}, \quad (1)$$

where $\mathbf{s} \in \mathbb{C}^N$ has only K_s ($K_s < N$) nonzero coefficients. CS theory states that although only a small number of measurements \mathbf{z} are collected:

$$\mathbf{z} = \Phi \mathbf{y} = \Phi \Psi \mathbf{s} = \mathbf{A} \mathbf{s}, \quad (2)$$

where $\Phi \in \mathbb{R}^{M \times N}$ is an $M \times N$ ($K_s < M < N$) sensing matrix, an overwhelming probability to accurately reconstruct \mathbf{s} from \mathbf{z} holds, if $\mathbf{A} = \Phi \Psi$ satisfies the restricted isometry property (RIP) [2]. The sparseness-promoting problem:

$$\min \|\mathbf{s}\|_0 \text{ s.t. } \mathbf{y} = \Psi \mathbf{s} \quad (3)$$

is an NP-complete problem. The convex relaxed version [2] of Eq. (3) bypasses the computational difficulty by replacing the l_0 norm with the l_1 norm and also guarantees correct reconstructions if certain conditions, such as RIP, for the equivalent sensing matrix \mathbf{A} are satisfied. However, convex solvers encounter notable computational complexity for large scale problems. The significant delay introduced will hinder applications which demand fast reconstruction and detection. Although convex solvers guarantee higher reconstruction accuracy, alternative greedy algorithms such as the Orthogonal Matching Pursuit (OMP) [7] and CoSaMP [8] offer advantages in terms of speed and ease of implementation. Particularly, in a dynamic CR context, fast spectrum detection plays a critically important role, hence motivating us to tailor new greedy pursuit techniques for the CR regime.

B. Nyquist rate Cyclic Feature Detection

The continuous cyclic autocorrelation function (CAF) for a second order cycstotatically signal $x(t)$ is defined by [9]:

$$\begin{aligned} R_{2x}^\alpha(\tau) &= \lim_{T \rightarrow \infty} \frac{1}{T} \int_{-T/2}^{T/2} u(t + \tau/2) \cdot v^*(t - \tau/2) dt \\ &= \frac{1}{T} \cdot u(\tau) * v^*(-\tau), \end{aligned} \quad (4)$$

where $u(t) = x(t)e^{-j\pi\alpha t}$, $v(t) = x(t)e^{j\pi\alpha t}$ and α denotes the cyclic frequency. The SCD, which are the Fourier coefficients of the CAF, is defined by:

$$S_{2x}^\alpha(f) = \mathcal{F}[R_{2x}^\alpha(\tau)] = \frac{1}{T} \cdot U(f) \cdot V^*(f), \quad (5)$$

where $U(f) = X(f + \frac{\alpha}{2})$ and $V(f) = X(f - \frac{\alpha}{2})$ are the frequency responses of $u(t)$ and $v(t)$ respectively. Eq.(5) unveils the nature of cyclic spectrum as a measurement of frequency correlation separated by α . The SCD can hence be obtained by time smoothing among the periodograms to achieve consistent estimation for Eq.(5), wherein the ‘time variant cross periodogram’ is defined by [9]:

$$I_{2x}^\alpha(t, f) = \frac{1}{T} X_T(t, f + \frac{\alpha}{2}) \cdot X_T^*(t, f - \frac{\alpha}{2}). \quad (6)$$

Here, $X_T(t, f)$ is the time-variant frequency response obtained using a window of length T . A classical nonsymmetric SCD estimator was proposed in [10] using ‘smoothed

periodograms’, that resorted to the convolution of the periodograms with a window function. This incurs difficulties in matrix formulations for a CS based approach, so alternatively we employ Welch’s method in a ‘sliding window’ manner to average periodograms within a temporal data range $T_1 = N \cdot K$, where N is the window length in samples and K denotes the total number of frames truncated. Therefore, we have the modified discrete estimation of SCD as:

$$S_{2x}[a, m] = \frac{1}{K \cdot N} \sum_{k=1}^K X_k[m+a] X_k^*[m-a], \quad (7)$$

where $\alpha = 2a \cdot \Delta f$ represents the cyclic frequency. Here Δf denotes the resolution of the N -dimensional Discrete Fourier Transform (DFT) coefficients $X_k[m]$, $0 \leq m \leq N-1$, which are computed using the k th truncated frame.

III. A NOVEL FRAMEWORK FOR SPARSER SCD

This section presents the proposed SCD estimator based on Welch’s method to facilitate the following model-based CS reconstruction. Rectangular windows are applied to sample the data.

Let $\mathbf{x}_k \in \mathbb{R}^N$ denote the k th frame of samples collected from $x(t)$ at sampling rate $f_s = f_n$, where N indicates the temporal window length and f_n corresponds to the Nyquist sampling rate. N should be chosen to be at least 3 to allow the conjugate symmetry [11] of the spectrum. The N -dimensional square Fourier matrix $\mathbf{D} \in \mathbb{C}^{N \times N}$ enables the DFT as:

$$\mathbf{f}_k = \mathbf{D} \mathbf{x}_k, \quad (8)$$

where $\mathbf{f}_k \in \mathbb{C}^N$ represents the Fourier coefficients of the k th frame. In order to avoid the spectrum from being folded as in [3], we need a spectrum centered at zero frequency. To achieve this goal, we exchange the block consisting of the first $N - \lfloor \frac{N}{2} \rfloor$ rows of \mathbf{D} with the block of the remaining $\lfloor \frac{N}{2} \rfloor$ rows, while we retain the notation \mathbf{D} .

We define the matrix \mathbf{S}_{2x} by reforming Eq.(7) as:

$$\mathbf{S}_{2x} = \frac{1}{K \cdot N} \sum_{k=1}^K \mathbf{f}_k (\mathbf{f}_k)^H. \quad (9)$$

The resultant matrix $\mathbf{S}_{2x} \in \mathbb{C}^{N \times N}$ consists of the SCD entries $s[i, j]$ on the i th row and j th column as:

$$s[i, j] = \frac{1}{K \cdot N} \sum_{k=1}^K \mathbf{f}_k[i] \cdot \mathbf{f}_k^*[j], \quad 1 \leq i, j \leq N. \quad (10)$$

Each entry in Eq.(10) is a scaled averaged discrete version of the periodogram defined by Eq.(6). The index difference $i - j$ for each entry $s[i, j]$ implies the spectral gap separating two correlated spectral components. In this way, entries on the same diagonal of \mathbf{S}_{2x} share the identical index difference $i - j$, and hence the same cyclic frequency $\alpha = 2a \cdot \Delta f = (i - j) \cdot \Delta f$, while entries on the same anti-diagonal $i + j$ refer to an identical frequency $\mathbf{f}_k[\frac{i+j}{2}]$.

Hence, the main diagonal of \mathbf{S}_{2x} in essence represents the f axis ($\alpha = 0$), while the minor diagonal indicates the α axis

($f = 0$). In order to ensure both a and $\frac{i+j}{2}$ are feasible integers, we only extract diagonals from the reconstructed \mathbf{S}_{2x} where $i - j$ is even for the post-recovery detection test. Owing to this decimation, the resolution of cyclic period is $\Delta\alpha = \frac{2f_n}{N}$, which halves the spectral resolution $\Delta f = \frac{f_n}{N}$.

We adopt the causal random sampler [12] in order to maintain the causality of the sampling process, in which the M rows of the sensing matrix $\Phi \in \mathbb{R}^{M \times N}$ are randomly selected from an identity matrix \mathbf{I}_N without changing the order of the rows. Let \mathbf{z}_k denote the random measurements vector with a reduced sampling rate $f_s = \frac{M}{N} f_n$:

$$\mathbf{z}_k = \Phi \mathbf{x}_k, \quad (11)$$

where $\frac{M}{N}$ is the compression rate. According to Eq.(9), \mathbf{S}_{2x} can be rewritten as:

$$\mathbf{S}_{2x} = \frac{1}{K \cdot N} \sum_{k=1}^K \mathbf{D} \mathbf{x}_k \mathbf{x}_k^T \mathbf{D}^H = \frac{1}{K \cdot N} \mathbf{D} \left(\sum_{k=1}^K \mathbf{x}_k \mathbf{x}_k^T \right) \mathbf{D}^H, \quad (12)$$

and it follows that:

$$\Phi \mathbf{D}^{-1} \mathbf{S}_{2x} (\mathbf{D}^H)^{-1} \Phi^T = \frac{1}{K \cdot N} \Phi \left(\sum_{k=1}^K \mathbf{x}_k \mathbf{x}_k^T \right) \Phi^T. \quad (13)$$

Note that $\mathbf{D}^H = N \cdot \mathbf{D}^{-1}$, which avoids the inverse manipulation of \mathbf{D} . Therefore, according to Eq.(11) and Eq.(13), we have:

$$\frac{1}{N^2} \Phi \mathbf{D}^H \mathbf{S}_{2x} \mathbf{D} \Phi^T = \frac{1}{K \cdot N} \sum_{k=1}^K \mathbf{z}_k \mathbf{z}_k^T. \quad (14)$$

Since $\text{vec}(\mathbf{ABC}) = (\mathbf{C}^T \otimes \mathbf{A}) \text{vec}(\mathbf{B})$, we obtain:

$$[(\mathbf{D} \Phi^T)^T \otimes \Phi \mathbf{D}^H] \text{vec}(\mathbf{S}_{2x}) = \frac{N}{K} \text{vec} \left(\sum_{k=1}^K \mathbf{z}_k \mathbf{z}_k^T \right). \quad (15)$$

This completes the new under-determined linear system:

$$\mathbf{A} \mathbf{s} = \mathbf{z}, \quad (16)$$

where $\mathbf{A} = \Phi \mathbf{D}^T \otimes \Phi \mathbf{D}^H$, $\mathbf{z} = \frac{N}{K} \text{vec} \left(\sum_{k=1}^K \mathbf{z}_k \mathbf{z}_k^T \right)$, and \mathbf{s} is the vectorized \mathbf{S}_{2x} .

Note that $\sum_{k=1}^K \mathbf{x}_k \mathbf{x}_k^T$ in Eq. (12) essentially represents the averaged covariance matrix without rotation, which contrasts with the use of the auxiliary autocorrelation matrix in [3]. Eq.(16) thus retains all useful temporal information, avoiding zero padding or the use of mapping matrices as in [3] and consequently, much alleviated spectral tails. The equivalent sensing matrix \mathbf{A} only necessitates the use of a DFT matrix, allowing a more straightforward temporal-spectral expression.

IV. CAPITALIZE ON MODEL-BASED CS: IMP

In view of the fact of the symmetry and cyclic patterns in SCD, multiple peak entries in matrix \mathbf{S}_{2x} jointly indicate the spectrum occupancy of the same user. The appearance of one user is thus reflected in the vector $\mathbf{s} = \text{vec}(\mathbf{S}_{2x})$ as a group of associated but scattered entries. We show in this section that

this characteristic is effectively equivalent to the block sparsity model [13] [14] with a certain block size d . Consequently, we can take advantage of the hidden block sparsity in solving Eq.(16), although we do not assume any block structure in the spectrum itself.

A. Block Sparsity Model Preliminaries

Considering the under-determined system Eq.(16), the unknown vector $\mathbf{s} \in \mathbb{C}^{\hat{N}}$ can be partitioned as a concatenation of blocks $\mathbf{s}^T[J]$, $J = 1 \cdots \widehat{M}$

$$\mathbf{s} = \left[\underbrace{s_1 \cdots s_d}_{\mathbf{s}^T[1]} \underbrace{s_{d+1} \cdots s_{2d}}_{\mathbf{s}^T[2]} \cdots \underbrace{s_{\widehat{N}-d+1} \cdots s_{\widehat{N}}}_{\mathbf{s}^T[\widehat{M}]} \right]^T, \quad (17)$$

where d denotes the block size and $\widehat{M} = \widehat{N}/d$ is the total number of blocks, the sensing matrix \mathbf{A} can be similarly partitioned into concatenated column-blocks $\mathbf{A}[J]$, $J = 1 \cdots \widehat{M}$:

$$\mathbf{A} = \left[\underbrace{\mathbf{a}_1 \cdots \mathbf{a}_d}_{\mathbf{A}[1]} \underbrace{\mathbf{a}_{d+1} \cdots \mathbf{a}_{2d}}_{\mathbf{A}[2]} \cdots \underbrace{\mathbf{a}_{\widehat{N}-d+1} \cdots \mathbf{a}_{\widehat{N}}}_{\mathbf{A}[\widehat{M}]} \right]. \quad (18)$$

The signal \mathbf{s} is called ‘block K_s -sparse’ if it contains only at most K_s blocks with nonzero Euclidean norm.

It is proved in [13] that both the block coherence

$$\mu_B = \max_{1 \leq J_1 \neq J_2 \leq \widehat{M}} \frac{1}{d} \|\mathbf{A}^*[J_1] \mathbf{A}[J_2]\|, \quad (19)$$

and the sub-coherence:

$$\nu = \max_{1 \leq l \leq \widehat{M}} \left(\max_{(l-1)d+1 \leq i \neq j \leq ld} \|\mathbf{a}_i^* \mathbf{a}_j\|_1 \right), \quad (20)$$

are substantially smaller than the conventional coherence

$$\mu = \max_{1 \leq i \neq j \leq \widehat{N}} \frac{1}{d} \|\mathbf{a}^*[i] \mathbf{a}[j]\|. \quad (21)$$

‘Block sparse’ signal reconstruction hence can be guaranteed with an eased requirement for the equivalent sensing matrix, comparing to the reconstruction with the conventional CS model.

B. Interdependent Matching Pursuit (IMP)

We are now motivated to cluster the associated SCD entries in $\mathbf{s} \in \mathbb{C}^{N^2}$ into a block structured equivalent $\mathbf{s}_b \in \mathbb{C}^{N^2}$, in which one block only contains supports owing to one user of the spectrum. We hence introduce a unitary permutation matrix $\mathbf{P} \in \mathbb{R}^{N^2 \times N^2}$ with the aim of permutating \mathbf{s} into a block sparse vector $\mathbf{s}_b = \mathbf{P} \mathbf{s}$. The permutation matrix \mathbf{P} is all zeros except for a sole ‘1’ at each row and each column (i.e., an orthonormal basis). Hence, the column index of each sole ‘1’ from the first row through the N^2 th row sequentially indicates the desired order of the entries taken from \mathbf{s} to be put into \mathbf{s}_b . Based on the property of unitary matrices, we derive:

$$\mathbf{z} = \mathbf{A} \mathbf{s} = \mathbf{A} \mathbf{P}^{-1} \mathbf{P} \mathbf{s} = \mathbf{A} \mathbf{P}^T \mathbf{P} \mathbf{s} = \mathbf{A} \mathbf{P}^T \mathbf{s}_b, \quad (22)$$

where $\mathbf{s}_b = \mathbf{P} \mathbf{s}$ is a potential block sparse vector associated with the new projection matrix $\mathbf{A} \mathbf{P}^T$, while $\mathbf{A} \mathbf{P}^T = (\mathbf{P} \mathbf{A}^T)^T$

Algorithm 1 Interdependent Matching Pursuit

Input: Sensing matrix \mathbf{A} , model-based function \mathbb{J} , permutation matrix \mathbf{P} , measurements vector \mathbf{z}

Initialization: $t = 0$, $\mathbf{s}_0 = \mathbf{0}$, $\mathbf{r}_0 = \mathbf{z}$, $\mathcal{Q}_0 = \phi$, $\mathbf{A}_0 = \phi$;

while halting criterion false **do**

$t = t + 1$;

$J_t = \arg \max_J \left\| (\mathbf{A}\mathbf{P}^T)^H [J] \mathbf{r}_{t-1} \right\|_2$;

$\widehat{\mathbf{A}}_t = (\mathbf{A}\mathbf{P}^T)[J_t]$, $\mathbf{A}_t = [\mathbf{A}_{t-1} \ \widehat{\mathbf{A}}_t]$, $\mathcal{Q}_t = \mathcal{Q}_{t-1} \cup J_t$;

$\mathbf{s}_t = \mathbf{A}_t^\dagger \mathbf{z}$;

$\mathbf{r}_t = \mathbf{z} - \mathbf{A}_t \mathbf{s}_t$; (\mathbf{r}_t is the residual)

end while

$\mathbf{s}_{b, \mathcal{Q}_t} = \mathbf{s}_t$, $\mathbf{s}_{b, \overline{\mathcal{Q}}_t} = \mathbf{0}$;

return $\widehat{\mathbf{s}} = \mathbf{P}^T \mathbf{s}_b$;

permutes the columns of \mathbf{A} in exactly the same order as in \mathbf{s}_b .

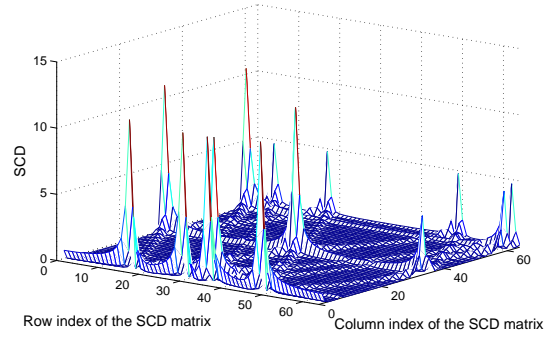
The format of the permutation matrix \mathbf{P} depends on the desired order of the entries to be clustered. This order in fact is fixed and is only determined by the embedded symmetry of \mathbf{S}_{2x} as well as the presented cyclic features owing to the modulation type. The block size is denoted as d , while we denote the modulation type related model function as \mathbb{J} which is stated in the following Lemma 1 and Lemma 2. The indices to be included in each block is grouped as $\mathcal{J} = \{j_1, \dots, j_d\} = \mathbb{J}(j_1)$, where there are total of $\frac{N^2}{d}$ such grouped blocks in \mathbf{s}_b . Note that the remaining indices $\{j_2, \dots, j_d\}$ are determined by function \mathbb{J} given any arbitrary entry index j_1 in \mathbf{s} . \mathbf{P} is thus readily obtained with the goal to permute all N^2 entries in \mathbf{s} into a concatenation of blocks according to the block-oriented permutation determined by \mathbb{J} . As a result, by sequentially computing $\mathcal{J} = \mathbb{J}(j_1)$ for $j_1 = 1, \dots, N^2$, all entries in \mathbf{s} are clustered into a block structured \mathbf{s}_b , where a single block $\mathbf{s}_b[J]$ actually consists of the entries indexed by a $\mathcal{J} = \{j_1, \dots, j_d\}$ in \mathbf{s} , which corresponds to symmetrical replicas and cyclic features owing to a single spectrum user. The indices that have been included in previous blocks must not be processed again as initial new j_1 for subsequent block computations $\mathbb{J}(j_1)$ and so are jumped.

Lemma 1. *The $\mathbf{s} = \text{vec}(\mathbf{S}_{2x})$ is conjugate symmetrical about $\mathbf{s}[\frac{N^2+N+2}{2}]$ for even N and $\mathbf{s}[\frac{N^2+1}{2}]$ for odd N regardless of the modulation type, giving $d = 2$ and interdependent indices pair $\{j_1, j_2\}$, where $j_2 = N^2 + N + 2 - j_1$ (N even), and $j_2 = N^2 + 1 - j_1$ (N odd). Here j_1 is an arbitrary entry index for \mathbf{s} .*

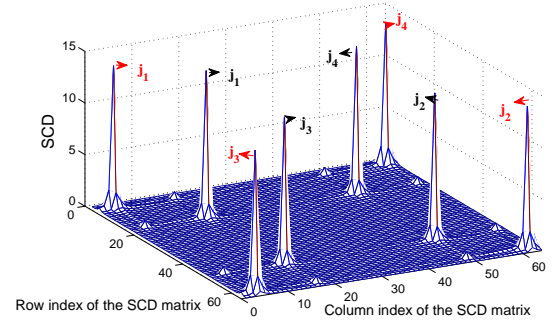
Lemma 1 stems from the conjugate symmetric nature of the DFT coefficients for a real discrete signal: $X_k[m] = X_k^*[N - m]$, $1 \leq m \leq N - 1$ [11]. Regarding the fold-free $\mathbf{f}_k[i]$ in Eq.(8) yields:

$$\mathbf{f}_k[i] = \mathbf{f}_k^*[2 \cdot \left\lfloor \frac{N}{2} \right\rfloor + 2 - i], \quad 2 \leq i \leq N, \quad (23)$$

which states that \mathbf{S}_{2x} is symmetrical about the main diagonal and conjugate symmetrical about the minor-diagonal according



(a) Absolute values of the constructed SCD by Tian's approach (noiseless, $M/N = 1$, $N = 64$).



(b) Absolute values of the constructed SCD by the proposed scheme (noiseless, $M/N = 1$, $N = 64$).

Fig. 1. Comparison of the constructed SCD for 2 BPSK spectrum users.

to Eq.(10). The symmetry present in \mathbf{S}_{2x} is thus reflected in its vectorized representation $\mathbf{s} = \text{vec}(\mathbf{S}_{2x})$ as in Lemma 1¹. Lemma 1 unveils the hidden block sparse nature behind \mathbf{s} with $d = 2$. To further reduce the degree of freedom, multiple cyclic features owing to one user also contribute to an increase of d . Take for instance, if a BPSK signal is present at $f = \pm f_c$, spectral peaks simultaneously appear at cyclic frequencies $\alpha = \pm 2f_c$ [9].

Lemma 2. *For a BPSK modulated signal, the block size increases to $d = 4$ owing to the presence of the cyclic frequency $\alpha = \pm 2f_c$, giving additional associated indices j_3 and j_4 , where $j_3 = 2 \lfloor \frac{N}{2} \rfloor + 2 - (j_1 - 2 \lfloor j_1/N \rfloor \cdot N)$, $j_4 = 2 \lfloor \frac{N}{2} \rfloor + 2 - (j_2 - 2 \lfloor j_2/N \rfloor \cdot N)$.*

We illustrate Lemma 1 and Lemma 2 in Fig. 1(b) where two BPSK signals are present in the novel SCD. According to the format in Eq.(10), the main diagonal of \mathbf{S}_{2x} represents the f axis ($\alpha = 0$), while the minor diagonal indicates the α axis ($f = 0$). The four peaks identified by black arrows are associated with one user and four peaks indicated with red the other. The locations of the cyclic frequency $\alpha = \pm 2f_c$ are indexed by j_3 and j_4 in \mathbf{s} . The peaks specified by j_1 and j_3 are present in one column in \mathbf{S}_{2x} with the symmetry about the $\lfloor \frac{N}{2} \rfloor + 1$ th row, while a similar relationship applies for the pair $\{j_2, j_4\}$ in a different column. In other words,

¹For even N , the first row and column are affected by $\mathbf{f}_k[1]$ and $\mathbf{f}_k^*[1]$ which are asymmetric [11], so we manually allocate $\mathbf{f}_k[1]$ as unoccupied to eliminate the effect.

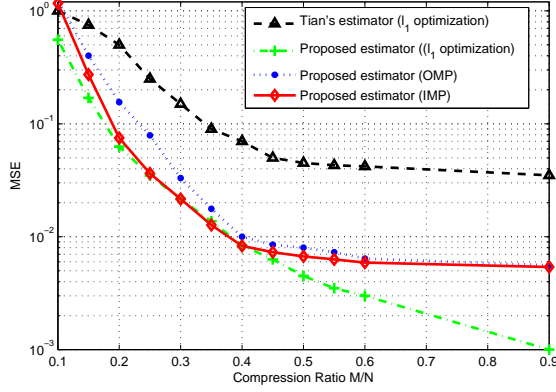


Fig. 2. MSE performance comparison for SCD reconstruction (spectrum occupancy=0.08).

$\lfloor j_1/N \rfloor = \lfloor j_3/N \rfloor$, $\lfloor j_2/N \rfloor = \lfloor j_4/N \rfloor$, while $\text{mod}(j_3, N) + \text{mod}(j_1, N) = 2 \lfloor \frac{N}{2} \rfloor + 2$ and $\text{mod}(j_4, N) + \text{mod}(j_2, N) = 2 \lfloor \frac{N}{2} \rfloor + 2$, which gives Lemma 2. The spectral occupancies in the SCD matrix \mathbf{S}_{2x} hence imply two potentially occupied blocks with block size $d = 4$ in $\mathbf{s}_b = \mathbf{P} \cdot \text{vec}(\mathbf{S}_{2x})$. We do not include the effect of symbol rate in Lemma 2, since they are highly dependent on the design of the pulse-shaping filter.

In this way, we apply block selection to carry out IMP which is summarized as Algorithm 1. We select the J th block $\mathbf{A}\mathbf{P}^T[J]$ on the new basis $\mathbf{A}\mathbf{P}^T$ which is most correlated to the residual \mathbf{r}_{t-1} in iteration t :

$$J_t = \arg \max_J \left\| (\mathbf{A}\mathbf{P}^T)^H [J] \mathbf{r}_{t-1} \right\|_2, \quad (24)$$

and record the J_t sequentially in the growing set \mathcal{Q}_t . The pseudo-inverse step guarantees an orthogonal space in iteration t against the selected supports obtained in iteration $t-1$. The step $\mathbf{s}_{b, \mathcal{Q}_t} = \mathbf{s}_t$ means that the entries of \mathbf{s}_b whose indices are from the blocks recorded in set \mathcal{Q}_t are sequentially set to be equal to the components in \mathbf{s}_t , while $\mathbf{s}_{b, \overline{\mathcal{Q}_t}} = \mathbf{0}$ sets all other entries in \mathbf{s}_b to zeros. IMP finally returns $\tilde{\mathbf{s}}$ as the reconstruction of \mathbf{s} . Upon available information concerning the maximum number of users, a halting criterion can be chosen based on desired residual level or sparsity level. Cross validation techniques can also be integrated to estimate the sparsity level adaptively [15], however this is not the focus of this paper.

V. SIMULATION RESULTS

We simulate a wideband spectrum of bandwidth 500MHz ($f_n = 1\text{GHz}$), occupied with 2 primary BPSK signals. The PUs appear randomly within the 500MHz range with symbol rate $f_{sb} = 16.8\text{MHz}$. By using a root raised cosine filter with roll-off factor $r = 0.5$, we have a spectrum occupancy of 0.08. The window length for SCD estimation is set to $N = 64$ samples per frame, with a total number of $K = 200$ frames. We use L to indicate the total number of rounds of the experiment. The MSE adopts the convention $\|\mathbf{s} - \tilde{\mathbf{s}}\|_2^2 / \|\mathbf{s}\|_2^2$, where \mathbf{s} indicates the original vectorized Nyquist SCD entries $\mathbf{s} = \text{vec}(\mathbf{S}_{2x})$ and $\tilde{\mathbf{s}}$ is the reconstructed vector.

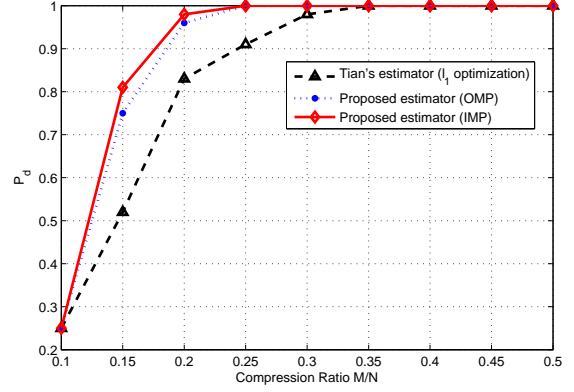


Fig. 3. Probability of detection (spectrum occupancy=0.08, false alarm rate $P_f = 0.01$).

A. A sparser SCD construction

Fig. 1(a) presents the Nyquist rate SCD estimator using [3] in contrast to the proposed estimator in Fig. 1(b). We use the integer notion [1,64] to index the axis of SCD in order to demonstrate the same 64×64 2D support without decimation as shown in Fig. 1(b). By using the proposed estimator, the spectral tail due to truncation is perfectly suppressed, resulting in a much sparser 2D SCD support than that of Tian's. Under the same spectrum occupancy of 0.08, the proposed estimator retains all temporal entries while it avoids any manual rotation or truncation regarding the symmetrical entries in the SCD or covariance matrix. This contrasts with the work in [3] which omits symmetric patterns and fills in the resultant vacancies with zeros in the auxiliary covariance matrix. For the sake of CS reconstruction, this sparsity potentially guarantees a more accurate signal recovery.

B. Noise-free SCD reconstruction

Fig. 2 highlights the MSE performance based on the new estimator in contrast to that of Tian's. In addition, OMP and IMP are also compared with $L = 200$ rounds for reconstruction. We extract certain diagonals from the SCD for spectrum detection according to Section III. Hence, to achieve the same cyclic spectrum resolution during PU detection, our window length should be twice the size of Tian's. Hence, we implement Tian's estimator with $N = 32$ and use $N = 64$ for the proposed estimator to evaluate the performance. Reconstructing on a much sparser SCD support, the proposed estimator leads to higher recovery accuracy as the compression ratio M/N varies from 0.1 to 0.9. We observe that the MSE performance of IMP approaches that of the convex solver while it has the much lower computational complexity of greedy pursuit. The gap between OMP and IMP diminishes as M/N increases. This is consistent with [13] which observes that the dominant bottleneck of the reconstruction shifts from undersampling to the true sparsity level of the signal once enough samples have been acquired.

The MSE floor in Fig. 2 essentially differs from the compression wall in [4]. Our result stems from the finite number of iterations of the greedy algorithm for a 'near sparse'

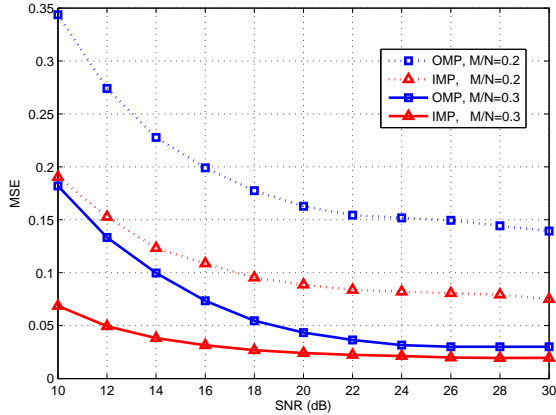


Fig. 4. MSE comparison for IMP and OMP against background noise (spectrum occupancy=0.08).

signal, while the floor in [4] is attributed to the non-unique solution caused by the introduced matrix regularization. If the reconstruction is performed by an l_1 based convex solver, the proposed framework breaks MSE floor as shown as Fig. 2.

With a finite number of K averaged frames, the SCD can be only reconstructed with errors owing to its ‘near sparse’ nature. The existing Generalized Likelihood Ratio Test (GLRT) [10] method thus no longer fits the statistics gained from the imperfect SCD. We instead apply the proposed test model in [4], where the distribution of the test statistic under the null hypothesis H_0 ‘the channel is idle’ is estimated first and then used to determine a threshold Γ . This distribution gives reference to a certain false alarm rate according to the threshold, namely $P_F = \Pr(\Lambda > \Gamma | H_0)$. The probability of detection is then yielded by the probability $P_D = \frac{1}{L} \sum n_{det} / n_{true}$ under a certain P_F , where n_{true} is the actual number of channels occupied in each round of experiment, and n_{det} is defined as the number of detected users according to the threshold. Fig. 3 illustrates that by employing a more reliable SCD reconstruction, the probability of detection P_d is correspondingly improved, at a fixed false alarm rate $P_f = 0.01$.

C. Robustness against noise

To evaluate the robustness of IMP against noise, we account for measurement error and spectrum background noise by adding a zero mean uncorrelated Gaussian noise \mathbf{n} to the model. This gives the model $\mathbf{z} = \mathbf{A}\mathbf{s} + \mathbf{n}$, upon which we carry out $L = 200$ round experiments with regard to SNR for certain fixed compression ratios. The received signal to noise ratio SNR is defined as $\text{SNR} = 10 \log_{10} \frac{\|\mathbf{z} - \mathbf{n}\|_2^2}{\|\mathbf{n}\|_2^2}$, while the definition of MSE remains unchanged. This implies that we do not treat the wideband background noise as actual signal to be reconstructed but rather a disturbance added to the measurements. Fig. 4 shows the superior recovery of IMP at $M/N = 0.2$ and 0.3 , which verifies the lower error bound guaranteed in [14] with $d = 4$. IMP selects 4 supports at each iteration, yielding an averaged reconstruction time 0.1197s ($M/N = 0.2$) and 0.4324s ($M/N = 0.3$) in our Matlab

simulation, which is about 4 times better than we achieved by using conventional OMP. This demonstrates the negligible overhead introduced by \mathbf{P} . The performance gap between the two grows significantly as the SNR decreases. Especially in the range of SNR from 10 to 15 dB when conventional greedy pursuit becomes vulnerable to disturbance, the model-based IMP exhibits robust noise tolerance with slower performance degradation, showing strong evidence of a reduced degree of freedom based on the block sparse model \mathbb{J} .

VI. CONCLUSION

In this paper, we propose a novel CS-enhanced cyclostationarity based spectrum sensing framework associated with a novel spectrum reconstruction algorithm IMP. We attribute the recovery superiority and performance guarantee of the proposed approach to the hidden block sparse nature and verify its performance via simulations. Our future work includes a theoretical analysis for the statistical test on the lossy SCD reconstruction in lower SNR scenarios.

REFERENCES

- [1] E. Axell, G. Leus, E. Larsson, and H. Poor, “Spectrum sensing for cognitive radio : State-of-the-art and recent advances,” *Signal Processing Magazine, IEEE*, vol. 29, no. 3, May 2012.
- [2] E. J. Candès, “Compressive sampling,” in *Proceedings of the International Congress of Mathematicians*, Madrid, Spain, 2006.
- [3] Z. Tian, Y. Tafesse, and B. Sadler, “Cyclic feature detection with subnyquist sampling for wideband spectrum sensing,” *Selected Topics in Signal Processing, IEEE Journal of*, vol. 6, no. 1, Feb. 2012.
- [4] E. Rebeiz, V. Jain, and D. Cabric, “Cyclostationarity-based low complexity wideband spectrum sensing using compressive sampling,” in *Communications (ICC), 2012 IEEE International Conference on*, Ottawa, Canada, June 2012.
- [5] Z. Khalaf, A. Nafkha, and J. Palicot, “Blind spectrum detector for cognitive radio using compressed sensing,” in *Global Telecommunications Conference (GLOBECOM), 2011 IEEE*, Dec. 2011.
- [6] R. Baraniuk, V. Cevher, M. Duarte, and C. Hegde, “Model-based compressive sensing,” *Information Theory, IEEE Transactions on*, vol. 56, no. 4, pp. 1982–2001, april 2010.
- [7] J. Tropp and A. Gilbert, “Signal recovery from random measurements via orthogonal matching pursuit,” *Information Theory, IEEE Transactions on*, vol. 53, no. 12, Dec. 2007.
- [8] D. Needell and J. Tropp, “CoSamp: Iterative signal recovery from incomplete and inaccurate samples,” *Applied and Computational Harmonic Analysis*, vol. 26, no. 3, pp. 301 – 321, 2009.
- [9] W. Gardner, “Exploitation of spectral redundancy in cyclostationary signals,” *Signal Processing Magazine, IEEE*, vol. 8, no. 2, April 1991.
- [10] A. Dandawate and G. Giannakis, “Statistical tests for presence of cyclostationarity,” *Signal Processing, IEEE Transactions on*, vol. 42, no. 9, Sep 1994.
- [11] A. V. Oppenheim, R. W. Schaffer, and J. R. Buck, *Digital Signal Processing*. New Jersey: Prentice Hall, 1998.
- [12] W. Chen and I. Wassell, “Energy-efficient signal acquisition in wireless sensor networks: a compressive sensing framework,” *Wireless Sensor Systems, IET*, vol. 2, no. 1, pp. 1–8, 2012.
- [13] Y. Eldar, P. Kuppinger, and H. Bolcskei, “Block-sparse signals: Uncertainty relations and efficient recovery,” *Signal Processing, IEEE Transactions on*, vol. 58, no. 6, pp. 3042–3054, june 2010.
- [14] Z. Ben-Haim and Y. Eldar, “Near-oracle performance of greedy block-sparse estimation techniques from noisy measurements,” *Selected Topics in Signal Processing, IEEE Journal of*, vol. 5, no. 5, pp. 1032–1047, sept. 2011.
- [15] H. Sun, A. Nallanathan, J. Jiang, and H. V. Poor, “Compressive autonomous sensing (CAsE) for wideband spectrum sensing,” in *Communications (ICC), 2012 IEEE International Conference on*, Ottawa, Canada, June 2012.